

Thermal kinetics analysis of coal-gangue selected from Inner Mongolia in China

Yunpeng Wang¹ · Yongfeng Zhang¹ · Quan Zhou¹ · Yinmin Zhang¹ · Junmin Sun¹

Received: 10 April 2017 / Accepted: 12 August 2017 / Published online: 23 August 2017
© Akadémiai Kiadó, Budapest, Hungary 2017

Abstract Thermal behavior and kinetics analysis of coal-gangue sample selected from Inner Mongolia Autonomous Region in China were investigated by using thermogravimetry–derivative thermogravimetry, X-ray diffraction (XRD) analysis, and Fourier transform infrared (FT-IR) spectroscopy. The mineralogy of coal-gangue was mainly determined as kaolinite, quartz, and boehmite. The XRD and FT-IR results showed that the structure change in coal-gangue with the temperature increased. The structure parameters of the microcrystal carbon in coal-gangue sample, including interlayer spacing (d_{002}), average lateral sizes (L_a), stacking heights (L_c), and aromaticity (f_a), were calculated based on XRD data. With the increase in temperature, the values of d_{002} and L_a decreased from 3.982 and 0.223 to 3.373 and 0.198 nm, respectively; however, the values of L_c and f_a increased from 0.111 and 0.633 to 0.156 and 0.852 nm, respectively. The average activation energy of coal-gangue was 102.66 and 103.73 kJ mol⁻¹, respectively, based on the Coats–Redfern and Flynn–Wall–Ozawa method.

Keywords Coal-gangue · Thermal behavior · Microcrystal carbon · Kinetic

Introduction

Coal-gangue is generated from the process of mining and beneficiation of coal, which accounts for approximately 10–15 mass% of coal production [1]. Coal-gangue, as one

of the largest sources of industrial solid waste in china, causes damage to environment, including acid drainage, heavy metals leaching as well as atmospheric pollution [2, 3]. Coal-gangue usually could be used as an energy material due to its certain heating values. The combustion behavior of coal-gangue has been investigated in previous studies [4, 5]. Many investigations focused on the effect of various atmospheric conditions on the ignition performance, the combustion performance, and the kinetic parameters of coal-gangue selected from different regions. Meng et al. found that combustion behavior of coal-gangue in oxy-fuel condition differed from that in air condition, which showed that the ignition of coal-gangue in the CO₂/O₂ conditions is delayed compared to that in the N₂/O₂ condition [4]. Ren et al. have studied that characteristic combustion parameters of coal-gangue increased with decreasing O₂ concentrations, while the maximum and average combustion rates presented decreased tendency [6]. The mass loss decreased, while comprehensive combustion characteristic index increased slightly when CH₄ presented in the combustion atmosphere with equivalent O₂ concentration. Many studies pointed out that the combustible matter content had a significant effect on ignition and combustion of coal-gangue. The combustion behavior of high-ash coal-gangue is affected by both combustion conditions and structural properties. However, the effect mechanism of structural properties on coal-gangue combustion behavior is not very clear and need to be investigated. Different instrumental techniques, including X-ray diffraction (XRD) and Fourier transform infrared (FT-IR) spectroscopy, have been used to investigate the combustion behavior and transformation of coal-gangue heated at different conditions [7, 8]. The fraction of aromaticity (f_a), interlayer spacing of the crystalline structure (d_{002}), and crystallite sizes (L_a , L_c) have been used as structural

✉ Yinmin Zhang
pzqm163@163.com

¹ Chemical Engineering College, Inner Mongolia University of Technology, Hohhot 010051, China

parameters to evaluate the carbon stacking structure in carbon materials, which can be determined from the intensities of the characteristic diffraction peaks of coal-gangue [9].

In this paper, the thermal behavior of coal-gangue selected from Inner Mongolia Region in China was investigated by thermogravimetry–derivative thermogravimetry (TG–DTG), X-ray diffraction (XRD) analysis and Fourier transform infrared (FT-IR) spectroscopy, and the thermal kinetics parameters of coal-gangue sample were calculated by the Coats–Redfern and Ozawa–Flynn–Wall methods.

Experimental

Raw material

The raw coal-gangue sample used in this study was selected from Inner Mongolia Region in China. The sample was ground and sieved to particle size below 90 μm (170 mesh), and dried at 105 $^{\circ}\text{C}$ for 10 h. The chemical composition of the coal-gangue is SiO_2 , 34.58 mass%; Al_2O_3 , 31.95 mass%; Fe_2O_3 , 1.00 mass%; TiO_2 , 0.76 mass%; CaO , 0.3 mass%; Na_2O , 0.42 mass%; and K_2O , 0.02 mass%. The molar ratio of $\text{SiO}_2/\text{Al}_2\text{O}_3$ with 1.83 is less than the theoretical value of kaolinite. The ultimate and proximate data of coal-gangue sample are shown in Table 1. The 10 mg of raw coal-gangue sample was heated at different temperatures (100, 200, 300, 400, 500, 600, 700, 800 and 900 $^{\circ}\text{C}$, respectively) for 2 h at a rate of 10 $^{\circ}\text{C min}^{-1}$ in a muffle furnace under air atmosphere.

Characterization

The TG measurements were taken using a Netzsch-STA 409PC/PG thermogravimetric analyzer under the atmosphere of O_2/N_2 mixed gases (20/80%) with four different heating rates of 10, 15, 20, and 25 $^{\circ}\text{C min}^{-1}$, respectively. The flow rate of mixed gases was 100 mL min^{-1} .

The XRD patterns of samples were performed by using a Rigaku D/MAX 2500PC powder X-ray diffractometer with $\text{Cu K}\alpha$ radiation of 1.5406 nm operating at 40 kV and 150 mA. All the samples were scanned in a step-scan mode with the rate of 2 $^{\circ} \text{ min}^{-1}$ over the angular 2θ range of 4 $^{\circ}$ –60 $^{\circ}$.

Fourier transform infrared spectroscopy (FT-IR) is undertaken by a Nicolet 6700, Thermo Fisher. The number of scans accumulated was 32. The samples were prepared with potassium bromide (KBr) pellets (ca. 2% by mass in KBr). The FT-IR spectroscopy of prepared samples between 400 and 4000 cm^{-1} was recorded.

Kinetic modeling

Currently, the interest in determining the rate-dependent parameters of kinetic analysis of clay minerals using thermal analysis techniques increased. In this study, the thermal kinetic parameters of coal-gangue were investigated by the Coats–Redfern model and the Flynn–Wall–Ozawa method [10–12].

Coats–Redfern model

Coats–Redfern is an integral method, which is given by:

$$\ln \frac{G(\alpha)}{T^2} = \ln \frac{AR}{\beta E \left(1 - \frac{2RT}{E}\right)} - \frac{E}{RT}, \quad (1)$$

where A is the pre-exponential factor (s^{-1}), β is the heating rate ($\text{K}\cdot\text{s}^{-1}$), E is apparent activation energy (kJ mol^{-1}), R is the gas constant ($8.314 \text{ J K mol}^{-1}$), α is conversion rate, and $G(\alpha)$ is conversion function. The $G(\alpha)$ depends on the mechanism controlling the reaction and the size and shape of the reacting particles. Since it can be demonstrated that the expression $\ln[AR/\beta E (1 - 2RT/E)]$ is essentially constant for most values of E and range of combustion temperature [13], if the correct $G(\alpha)$ is used, the plot of $\ln[G(\alpha)/T^2]$ against $1/T$ should result in a straight line with a slope of $-E/R$, from which the values of E and A can be obtained.

Flynn–Wall–Ozawa model

Flynn–Wall–Ozawa model was derived from the integral method based on the following expression:

$$\ln(\beta) = \ln\left(\frac{AE}{RG(\alpha)}\right) - 5.331 - 1.052 \frac{E}{RT}. \quad (2)$$

From this equation, E can be estimated from the slope of the straight lines obtained by plotting $\ln(\beta)$ vs. $1/T$ at different conversion rates α [4, 14].

Table 1 Ultimate and proximate data of coal-gangue sample

	Ultimate/mass%					Proximate/mass%			
	C_{daf}	H_{d}	N_{d}	S_{d}	O_{d}	M_{ad}	A_{ad}	V_{ad}	FC_{ad}
Coal-gangue	58.36	6.69	9.25	2.74	31.28	0.38	71.63	13.60	14.39

Results and discussion

XRD analysis

The XRD pattern of the raw coal-gangue is shown in Fig. 1. As presented in Fig. 1, two symmetric diffraction peaks were observed at $2\theta = 12^\circ$ and $2\theta = 25^\circ$ with the values of 0.720 and 0.358 nm, respectively, which were attributed to the (001) and (002) of kaolinite ($\text{Al}_2\text{O}_3 \cdot 2\text{SiO}_2 \cdot 2\text{H}_2\text{O}$). Meanwhile, the other characteristic peaks with $d_{(003)} = 0.229$ nm and $d_{(060)} = 0.155$ nm for kaolinite were also observed [15–17]. The sharp and strong peaks with the values of 0.428 nm and 0.336 nm appeared approximately at $2\theta = 21^\circ$ and $2\theta = 27^\circ$ and were associated with quartz. In addition, the characteristic diffraction peaks for boehmite ($\gamma\text{-AlOOH}$) were found at $2\theta = 38^\circ$ and $2\theta = 55^\circ$. The result indicated that the mineralogy of the coal-gangue sample was determined as kaolinite, quartz, and a small amount of boehmite. Meanwhile, the presence of boehmite resulted in the decrease in molar ratio of $\text{SiO}_2/\text{Al}_2\text{O}_3$, which has a good consistency with the chemical composition.

The XRD patterns of coal-gangue samples heated at different temperatures are shown in Fig. 2. As shown in Fig. 2, the characteristic peaks for kaolinite presented no change before 400 °C. The intensities of characteristic peaks for quartz gradually increased, which may be associated with the combustion and removal of carbon [18]. The characteristic peaks of kaolinite disappeared when the temperature increased up to 500 °C, which was attributed to the dehydroxylation of kaolinite in coal-gangue [19]. The disappearance of characteristic peaks for boehmite ($\gamma\text{-AlOOH}$) and the presence of characteristic peaks for Al_2O_3 at approximately $2\theta = 33^\circ$ and $2\theta = 54^\circ$ indicated the

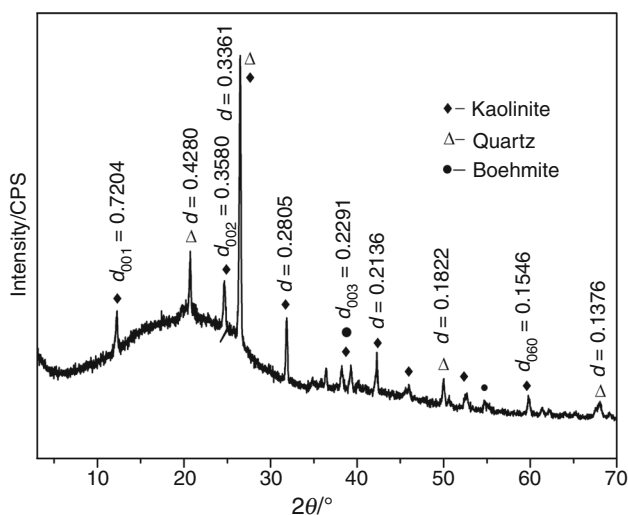


Fig. 1 XRD pattern of raw coal-gangue sample

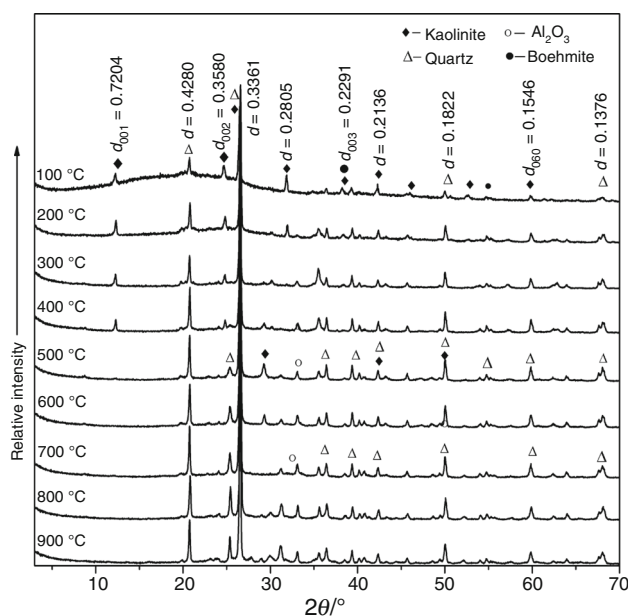
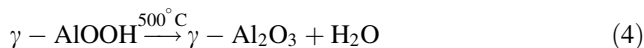
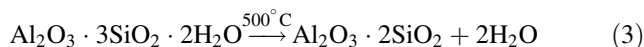


Fig. 2 XRD patterns of coal-gangue samples heated at different temperatures

dehydration of boehmite ($\gamma\text{-AlOOH}$) and the formation of $\gamma\text{-Al}_2\text{O}_3$ [16, 18]. When the temperature increased from 600 to 900 °C, the XRD patterns presented unobvious change and the mineral composition were mainly determined as quartz and $\gamma\text{-Al}_2\text{O}_3$. The details of these conversion reactions are as follows [4, 20, 21]:



The XRD patterns of coal-gangue samples heated from room temperature to 400 °C presented a relatively broad diffraction region that ranged from 10° to 35° , which indicated that coal-gangue contained microcrystalline carbon and the char structure with short range order. The peak fitting diagram of raw coal-gangue sample is shown in Fig. 3. The (002) diffraction peak indicated the space of aromatic ring layers and the aromatic layer stack structure of the microcrystal carbon. Yen and Sonibare considered that the (100) peak approximately at 40° was due to presence of saturated structure, which is attached to the edge of coal crystallites [22, 23]. The (λ) reflected the packing distance of saturated structures, which corresponded to the aromatic layer structure coupled with the aliphatic hydrocarbon side chain, various functional group, and aliphatic carbon microcrystalline. This aromaticity is usually used to describe the ratio of carbon atoms in aromatic rings vs aliphatic side chains. The γ peak was associated with the aliphatic side chains grafted on the edge of char crystallites. Theoretically, the areas of the γ and Π -peaks are

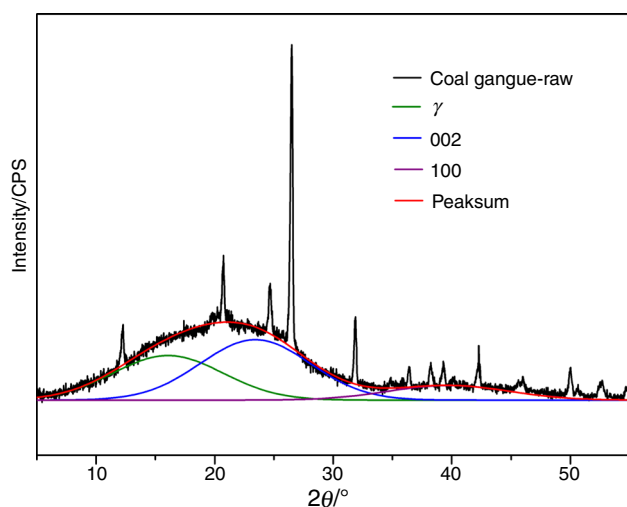


Fig. 3 Peak fitting diagram of raw coal-gangue sample

equal to the number of aromatic carbon atoms (C_{ar}) and aliphatic carbon atoms (C_{al}), respectively [8, 21]. The f_a is defined as the aromaticity of coal-gangue as in Eq (5) [24, 25].

$$f_a = \frac{C_{ar}}{C_{ar} + C_{al}} \times 100\% = \frac{A_{002}}{A_{002} + A_{\gamma}} \times 100\%, \quad (5)$$

where A is the area of corresponding peak, and Eq. (3) shows that aromaticity of coal-gangue increased as γ peak decreased.

The crystalline structure parameters of the carbon in coal-gangue sample were estimated based on the (002) and (100) diffraction peaks by using the Bragg equation and Scherrer equations (Eqs. (6)–(8)) [9, 24–26]:

$$d_{002} = \frac{\lambda}{3 \sin \theta_{002}}; \quad (6)$$

$$L_c = \frac{K\lambda}{\beta_{002} \cos \theta_{002}}; \quad (7)$$

$$L_a = \frac{K\lambda}{\beta_{100} \cos \theta_{100}}. \quad (8)$$

The λ is the wavelength of X-ray, which was 1.541 nm. The θ is the diffraction angle, θ_{002} is the angle of the (002) peak, d_{002} is the crystalline interplanar spacing, K is the shape factor of different peak, and β is the peak width at the half-maximum intensity of the (002) and (100) peaks. To calculate L_c and L_a , K values of 0.89 and 1.84 are used, respectively [27]. The crystallite size perpendicular to the basal plane represented by average stacking height (L_c) is obtained from the (002) reflection, whereas the crystallite size paralleling the basal plane, represented by average diameter (L_a), is calculated by using the (100) reflection corresponding to the a unit cell parameter. The crystalline parameters include interplanar spacing (d_{002}), average diameter (L_a), average stacking height (L_c), and aromaticity

(f_a) and are shown in Fig. 4. As shown in Fig. 4, the values of d_{002} and L_a decreased from 3.982 and 0.223 to 3.373 and 0.198 nm as the temperature increased, respectively. Simultaneously, the values of L_c and f_a presented an increased tendency and increased from 0.111 and 0.633 to 0.156 and 0.852 nm, respectively, when the temperature increased up to 400 °C. The results may be attributed to saturated structure attached to the aliphatic side chains slightly grafted on the edges of coal crystallites. The aliphatic side chains detach from coal crystallites as the temperature increased, which reduced the carbon skeleton in the aromatic plies and increased the value of aromaticity (f_a). The results indicated that the coal-gangue gradually increased the degree of graphitic structure as the temperature raised.

TG–DTG analysis

The TG–DTG curves of coal-gangue samples heated with different heating rates are presented in Fig. 5. As shown in TG curves, the thermal transition process of raw coal-gangue can be divided into three stages for interpreting the thermal mechanism. The first stage was in the range from 30 °C to approximately 320 °C. As the temperature increased, one widely endothermic peak presented at approximately 105 °C in the DTG curves, which indicated the loss of moisture and a small amount of volatile matters in the coal-gangue. A gradual increase in tendency was observed between 200 and 320 °C, which may be attributed to the oxygen physisorption and chemisorption before the onset of combustion [28–31]. The second stage was in the range from 320 to 600 °C. One strong endothermic peak was observed approximately at 500 °C in the DTG curves, which is attributed to the dehydroxylation [32]. Meanwhile, the intensity of the peak became stronger with the increase in heating rate. The characteristic temperatures, including the release temperature to volatile (T_s), the ignition temperature (T_{ig}), the temperature of maximum mass loss (T_{max}), and the burnout temperature (T_b), are shown in Table 2. The T_s , T_{ig} , T_{max} and T_b all gradually increased with increasing heating rate, and the result may be attributed to the time lag resulted from the conductive heat transfer at the high heating rate. The temperature distribution within the coal-gangue particles is homogeneous at a low heating rate, and thus, the reaction can proceed more sufficiently. The devolatilization, volatiles combustion, and volatiles–char combustion are partially or completely overlapped in this stage [18, 33]. The mass loss of the coal-gangue was very slight in the last stage above 600 °C, which indicated that the volatiles and char have been burned out. The reaction of combustion mainly occurs in the second stage, and the loss on ignition amounts to 26.32–28.08%.

Fig. 4 Crystalline parameters of coal-gangue as a function of temperature of heat treat temperature

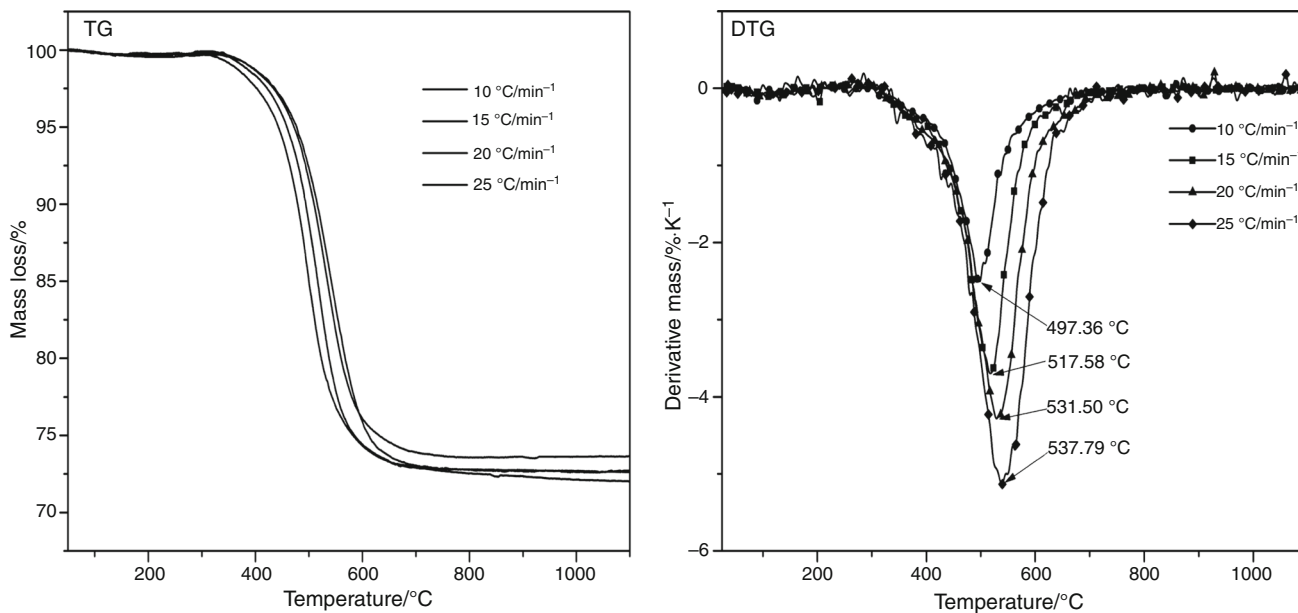
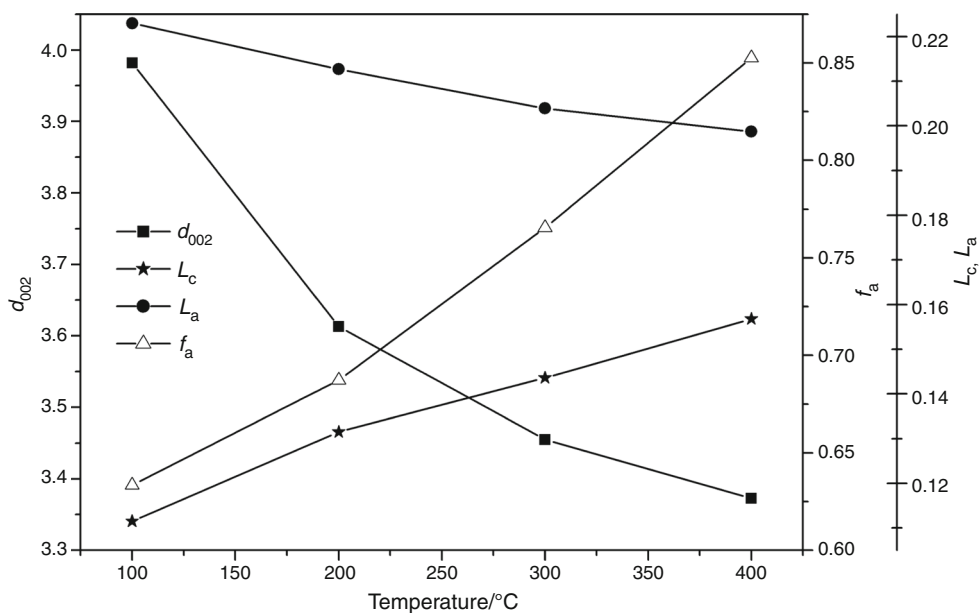


Fig. 5 TG/DTG curves for coal-gangue at different heating rates

Table 2 Combustion characteristic temperatures of coal-gangue sample

Heating rate/°C min ⁻¹	T_s /°C	T_{ig} /°C	T_{max} /°C	T_b /°C
10	308.13	445.43	491.06	549.24
15	321.18	460.20	518.48	563.57
20	325.70	465.05	529.03	577.90
25	335.34	472.71	539.62	599.58

FT-IR spectra analysis

The kaolinite contains inner and inner surface hydroxyls [18, 19, 34, 35]. The FT-IR spectrum of raw coal-gangue is presented in Fig. 6. As illustrated in Fig. 6, in the high-wavenumber region (4000–3000 cm⁻¹), two obvious bands were observed at 3693 and 3620 cm⁻¹, which were attributed to the stretching vibration modes of inner surface

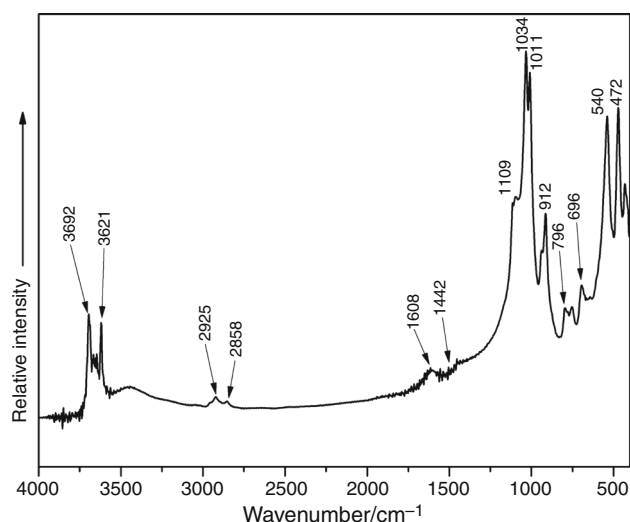


Fig. 6 FT-IR patterns of raw coal-gangue

hydroxyl and inner hydroxyl, respectively [16, 36, 37]. The intensity of the absorption band at 3693 cm^{-1} was stronger than that of the absorption band at 3620 cm^{-1} . The band at 3452 cm^{-1} was associated with the H–O–H vibration mode of water molecules [38]. However, the other two characteristic bands of kaolinite at 3668 and 3652 cm^{-1} in the high-wavenumber region do not appear, which indicated that the bottom surface structure of kaolinite in coal-gangue is imperfect [39]. The two characteristic vibration bands at 2925 and 2858 cm^{-1} were assigned to antisymmetric and symmetric stretching vibration modes of the CH_3 group [40]. In the wavenumber regions of $1700\text{--}400\text{ cm}^{-1}$, the band at 1608 cm^{-1} may be attributed to the vibration band of aromatic hydrocarbons or carboxylate salts. The band at 1442 cm^{-1} was associated with the methyl or methylene vibration mode. The presence of the two bands indicates that coal-gangue samples contain carbonaceous components. The bands at 1109 , 1034 , and 1011 were attributed to the symmetric stretching vibration of Si–O–Si. The band at 796 cm^{-1} was attributed to stretching vibration mode of inner hydroxyl [40, 41]. The band approximately at 696 cm^{-1} was associated with the stretching vibration mode of Si–O–Al, and the bands at 540 and 472 cm^{-1} were ascribed to the bending vibration mode of Si–O–Al [42–45].

The FT-IR spectra of samples heated at different temperatures are presented in Fig. 7a, b. The band at 3452 cm^{-1} disappeared at $200\text{ }^\circ\text{C}$ due to the removal of adsorption water. With the temperature increasing, the intensities of two bands at 3693 and 3619 cm^{-1} decreased slightly compared to that of raw coal-gangue, which disappeared and combined into a broad absorption band at $600\text{ }^\circ\text{C}$. The results were attributed to the dehydroxylation and indicated the phase transition of kaolinite to

metakaolin. The intensities of the bands at 912 and 593 cm^{-1} gradually decreased and disappeared at $600\text{ }^\circ\text{C}$, which was also attributed to the breakage of Al–OH and Si–O–Al as the temperature increased. The intensities of the band at 1033 and 1108 cm^{-1} also gradually weakened as the temperature increased, and a wide band was observed when the temperature reached $600\text{ }^\circ\text{C}$. The results were associated with the depolymerization and collapse of silica tetrahedron structure [16].

Thermal kinetics analysis

The single-heating-rate method and multiple-heating-rate method were highly reliable techniques for describing the kinetic analysis of thermal data [4, 6, 16, 46, 47]. The kinetics analysis of coal-gangue was investigated by using Coats–Redfern (C–R) method and Flynn–Wall–Ozawa (FWO) method based on TG–DTG data.

The kinetic curves of coal-gangue based on the FWO method are shown in Fig. 8, and the activation energy (E) values at different conversion rates (α) for coal-gangue sample are presented in Fig. 9. The kinetic parameters of coal-gangue sample based on Coats–Redfern and FWO method are presented in Tables 3 and 4. The higher E indicated that more energy was required in the process of coal-gangue combustion. As shown in Fig. 9, the E significantly increased with the increase in α , which reached the maximum value of $111.57\text{ kJ mol}^{-1}$ at $\alpha = 0.3$. Then, the E gradually decreased with the reduction in α . The reason for this phenomenon could be explained from two aspects. On the one hand, volatiles played a key role at the early stage of combustion. The relatively lower activation energy value at the beginning of the combustion process may be attributed to the existence of volatiles [4], which are more active and may more easily take part in the oxidation process. The significant increase in E when α increased from 0.1 to 0.3 was mainly attributed to the decrease in the volatile content in the devolatilization process and the presence of fixed carbon in the coal-gangue [4]. However, the decrease in E when α exceeds 0.3 may be ascribed to the intense combustion of fixed carbon. On the other hand, the combustion process of coal-gangue was affected by the catalysis of minerals presented in coal-gangue. Many researchers have found that clay minerals and pyrite can enhance the catalytic cracking and reduce the activation energy [48]. In this study, coal-gangue sample mainly contained kaolinite, quartz, and boehmite. Therefore, the decrease in E may also be attributed to the increase in the ash content in the process of combustion.

The average activation energy is an important kinetic parameter [49]. As shown in Tables 3 and 4, the average activation energies of coal-gangue samples calculated by the FWO method and the C–R method were 103.73 and

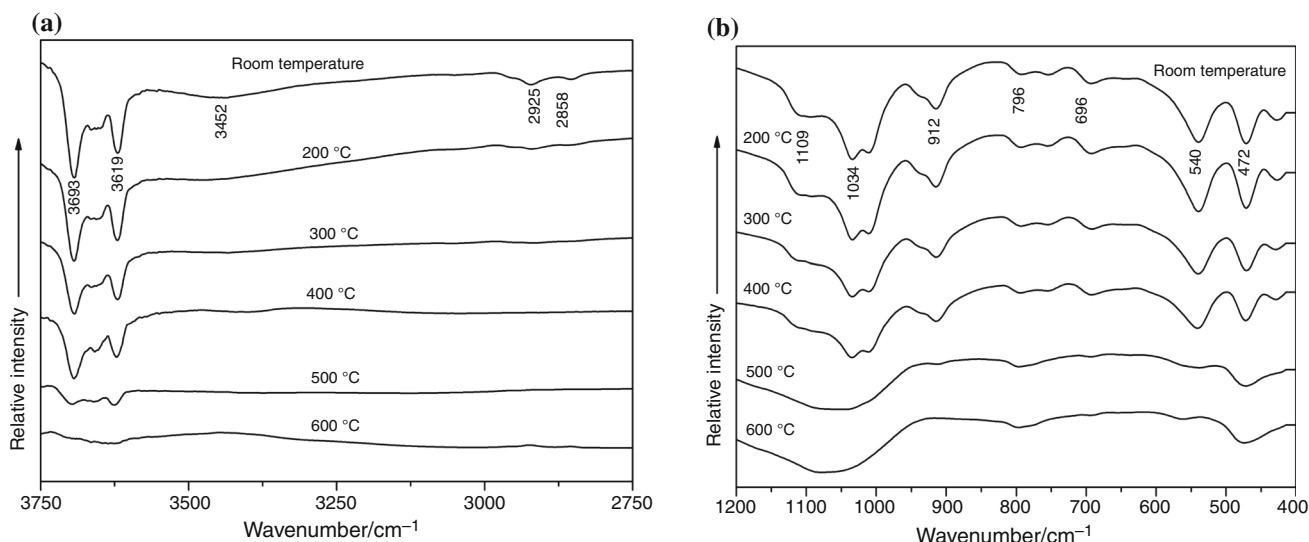


Fig. 7 FT-IR patterns of the coal-gangue samples heated at different calcined temperatures. **a** In the 400–1200 cm^{-1} region and **b** in the 2750–3750 cm^{-1} region

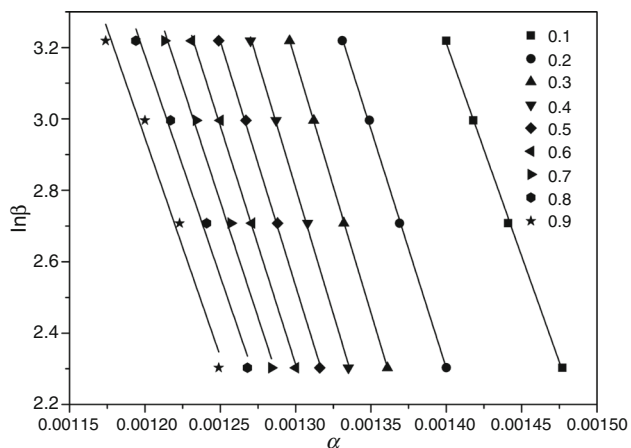


Fig. 8 Kinetic curves obtained by the FWO method corresponding to coal-gangue samples

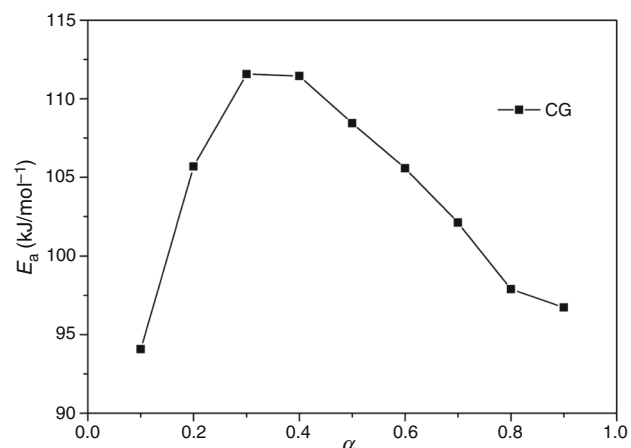


Fig. 9 Activation energy versus the degree of conversion corresponding to coal-gangue samples

Table 3 Kinetic parameters of coal-gangue sample based upon Coats–Redfern method

Heating rate/ $^{\circ}\text{C min}^{-1}$	$E/\text{KJ mol}^{-1}$	G/α	R^2
10	98.40	$-\ln(1 - \alpha)$	0.97107
15	105.25		0.96943
20	103.03		0.979
25	103.95		0.97925
Average	102.66		

Table 4 Kinetic parameters of coal-gangue sample based on FWO method

α	$E/\text{KJ mol}^{-1}$	R^2
0.1	94.07	0.99884
0.2	105.69	0.9992
0.3	111.57	0.99994
0.4	111.44	0.99855
0.5	108.44	0.99838
0.6	105.58	0.99799
0.7	102.12	0.9911
0.8	97.89	0.9858
0.9	96.73	0.9734
Average	103.73	

102.66 kJ mol^{-1} , respectively. The average activation energies obtained by both the methods are close. The results indicated that single-heating-rate method and multiple-heating-rate method are useful for analyzing coal-gangue combustion.

Conclusions

Thermal behavior and kinetics analysis of coal-gangue sample selected from Inner Mongolia Autonomous Region in China were investigated by using thermogravimetry–derivative thermogravimetry (TG–DTG), X-ray diffraction (XRD), and Fourier transform infrared (FT-IR) spectroscopy. The mineralogy of coal-gangue was determined as kaolinite, quartz, and boehmite. Meanwhile, the coal-gangue sample contains a small amount of amorphous carbon with turbostratic structure. The XRD and FT-IR spectra clearly showed the structure change in coal-gangue with the increase in temperature. The structure parameters of the microcrystal carbon in coal-gangue sample, including interlayer spacing (d_{002}), average lateral sizes (L_a), stacking heights (L_c), and aromaticity (f_a), were calculated based on XRD data. With the increase in temperature, the values of d_{002} and L_a decreased from 3.982 and 0.223 to 3.373 and 0.198 nm, respectively; however, the values of L_c and f_a increased from 0.111 and 0.633 to 0.156 and 0.852 nm, respectively. The average activation energies of coal-gangue were evaluated based on the Coats–Redfern and Flynn–Wall–Ozawa methods, which were 102.66 and 103.73 kJ mol⁻¹, respectively.

Acknowledgements The authors gratefully acknowledge the financial support by the National Natural Science Foundation of China (No. 51604158).

References

- Liu HB, Liu ZL. Recycling utilization patterns of coal mining waste in China. *Resour Conserv Recy*. 2010;54(12):1331–40.
- Querol X, Lzquierdo M, Monfort E, Alvarez E, Font O, Moreno T. Environmental characterization of burnt coal gangue banks at Yangquan, Shanxi Province, China. *Int J Coal Geol*. 2008;75(2):93–104.
- Ardejani FD, Shokri BJ, Bagheri M, Soleimani E. Investigation of pyrite oxidation and acid mine drainage characterization associated with Razi active coal mine and coal washing waste dumps in the Azad shahr-Ramian region, northeast Iran. *Environ Earth Sci*. 2010;61(8):1547–60.
- Meng FR, Yu JL, Tahmasebi A, Han Y. Pyrolysis and combustion behavior of coal gangue in O₂/CO₂ and O₂/N₂ mixtures using thermogravimetric analysis and a drop tube furnace. *Energy Fuels*. 2013;27(6):2923–32.
- Guo YX, Zhang YY, Cheng FQ. Industrial development and prospect about comprehensive utilization of coal gangue. *CIESC J*. 2014;65(7):2443–53.
- Ren Jun, Xie Chuanjin, Guo Xuan, Qin Zhifeng, Lin Jian-Ying, Li Zhong. Combustion characteristics of coal gangue under an atmosphere of coal mine methane. *Energy Fuels*. 2014;28(6):3688–95.
- Lu L, Sahajwalla V, Kong C, Harris D. Quantitative X-ray diffraction analysis and its application to various coals. *Carbon*. 2001;39(12):1821–33.
- Jiao Yong, Tian Wenjuan, Chen Huili, Shi Huangang, Yang Binbin, Li Chao, Shao Zongping, Zhu Zhenping, Li Si-Dian. In situ catalyzed Boudouard reaction of coal char for solid oxide-based carbon fuel cells with improved performance. *Appl Energy*. 2015;141:200–8.
- Zhang C, Yang XY, Li YF. Mechanism and structural analysis of the thermal activation of coal-gangue. *Adv Mat Res*. 2011;356–360:1807–12.
- Coats AW, Redfern JP. Kinetic parameters from thermogravimetric data. *Nature*. 1964;201(4914):68–9.
- Ozawa T. A new method of analyzing thermogravimetric data. *Bull Chem Soc Jpn*. 1965;38(11):1881–6.
- Flynn JH, Wall LA. A quick, direct method for the determination of activation energy from thermogravimetric data. *J Polym Sci B Polym Lett*. 1996;4(3):323–8.
- Gil MV, Casal D, Pevida C, et al. Thermal behaviour and kinetics of coal/biomass blends during Co-combustion. *Bioresour Technol*. 2010;101(14):5601–8.
- Hu RZ, Shi QZ. *Thermal analysis kinetics*. Beijing: Science Press; 2001.
- Bayram H, Mu E. Thermal analysis of a white calcium bentonite. *J Therm Anal Calorim*. 2010;101(3):873–9.
- Cheng H, Liu Q, Zhang J, Yang J, Frost RL. Delamination of kaolinite–potassium acetate intercalates by ball-milling. *J Colloid Inter Sci*. 2010;348(2):355–9.
- Cheng H, Zhou Y, Feng Y, Geng W, Liu Q, Guo W, et al. Electrokinetic energy conversion in self-assembled 2d nanofluidic channels with janus nanobuilding blocks. *Adv Mater*. 2017;29:1700177.
- Gong C, Dongxu LI, Wang X, Zongjin LI. Activity and structure of calcined coal gangue. *J Wuhan Univ Technol*. 2007;22(4):749–53.
- Ili Biljana R, et al. Thermal treatment of kaolin clay to obtain metakaolin. *Hem Ind*. 2010;64(4):351–6.
- Zhang Y, Nakano J, Liu L, Wang X, Zhang Z. Co-combustion and emission characteristics of coal gangue and low-quality coal. *J Therm Anal Calorim*. 2015;120(3):1883–92.
- Cheng H, Liu Q, Yang J, Frost RL. Thermogravimetric analysis of selected coal-bearing strata kaolinite. *Thermochim Acta*. 2010;507–508(33):84–903.
- Yen TF, Erdman JG, Pollack SS. Investigation of the structure of petroleum asphaltene by X-ray diffraction. *Anal Chem*. 2002;33(11):1587–94.
- Ming H. Modification of kaolinite by controlled hydrothermal deuteration—a DRIFT spectroscopic study. *Clay Miner*. 2004;39(3):349–62.
- Sonibare OO, Haeger T, Foley SF. Structural characterization of Nigerian coals by X-ray diffraction. *Fuel Energy Abstr*. 2010;35(12):5347–535.
- Lu L, Sahajwalla V, Kong C, Harris D. Quantitative X-ray diffraction analysis and its application to various coal. *Carbon*. 2001;39(12):1825–37.
- Qi Xuejun, Guo Xin, Xue Lucheng, Zheng Chuguang. Effect of iron on Shenfu coal char structure and its influence on gasification reactivity. *J Anal Appl Pyrol*. 2014;110(1):401–7.
- Li X, Zhu Z, Chen J, De Marco R, Dicks A, Bradley J, et al. Surface modification of carbon fuels for direct carbon fuel cells. *J Power Sources*. 2009;186(1):1–9.
- Zhang Y, Li J, Cheng F, Guo Y. Study of the combustion behavior and kinetics of different types of coal gangue. *Combust Explo Shock Waves*. 2015;51(6):70–677.
- Otero M, Diez C, Calvo LF, Garcia AI, Moran A. Analysis of the Co-combustion of sewage sludge and coal by TG–MS. *Biomass Bioenerg*. 2002;22(4):319–29.

30. Folgueras MB, Diaz RM, Xiberta J, Prieto I. Thermogravimetric analysis of the Co-combustion of coal and sewage sludge. *Fuel*. 2003;82(15):2051–5.
31. Yuzbasi NS, Selcuk N. Air and oxy-fuel combustion characteristics of biomass/lignite blends in TGA–FTIR. *Fuel Process Technol*. 2011;92(92):1101–8.
32. Cheng H, Yang J, Liu Q, He J, Frost RL. Thermogravimetric analysis–mass spectrometry (tg–ms) of selected Chinese kaolin-ites. *Thermochim Acta*. 2010;507–508:106–14.
33. Huang X, Jiang X, Han X, Wang H. Combustion characteristics of fine- and micro-pulverized coal in the mixture of O₂/CO₂. *Energy Fuel*. 2008;22(6):3756–62.
34. Cheng H, Liu Q, Cui X, Zhang Q, Zhang Z, Frost RL. Mechanism of dehydroxylation temperature decrease and high temperature phase transition of coal-bearing strata kaolinite intercalated by potassium acetate. *J Colloid Interface Sci*. 2012;376(1):47–56.
35. Zhang C, Yang XY, Li YF. Thermal treatment of coal-gangue: activation and relevant factors. *ICDMA*. 2010;2:843–8.
36. Cheng H, Liu Q, Yang J, Du X, Frost RL. Influencing factors on kaolinite–potassium acetate intercalation complexes. *Appl Clay Sci*. 2010;50(4):476–80.
37. Cheng H, Hou X, Liu Q, Li X, Frost RL. New insights into the molecular structure of kaolinite–methanol intercalation complexes. *Appl Clay Sci*. 2015;109–110:55–63.
38. Cheng H, Liu Q, Yang J, Ma S, Frost RL. The thermal behavior of kaolinite intercalation complexes—a review. *Thermochim Acta*. 2012;545:1–13.
39. Cheng H, Liu Q, Yang J, Zhang Q, Frost RL. Thermal behavior and decomposition of kaolinite–potassium acetate intercalation composite. *Thermochim Acta*. 2010;503–504:16–20.
40. Zhang YM, Liu QF, Wu ZG, Zheng QM, Cheng HF. Thermal behavior analysis of kaolinite–dimethylsulfoxide intercalation complex. *J Therm Anal Calorim*. 2011;111(3):1167–72.
41. Cheng HF, Li K, Liu QF, Zhang S, Li XG, Frost RL. Insight into the thermal decomposition of kaolinite intercalated with potassium acetate: an evolved gas analysis. *J Therm Anal Calorim*. 2011;117(3):1231–9.
42. Shiravand F, Fraga I, Cortés P, Calventus Y, Hutchinson JM. Thermal analysis of polymer layered silicate nanocomposites. *J Therm Anal Calorim*. 2014;118(2):723–9.
43. Frost RL, Johansson U. Combination bands in the infrared spectroscopy of kaolins; a DRIFT spectroscopic study. *Clay Miner*. 2004;46(3):466–77.
44. Li LX, Zhang YM, Zhang YF, Sun JM, Hao ZF. The thermal activation process of coal gangue selected from Zhungeer in China. *J Therm Anal Calorim*. 2016;118(2):723–9.
45. Cheng H, Xu P, Wang D, Frost RL. Thermal decomposition behavior and de-intercalation kinetics of kaolinite/quaternary ammonium salt complexes. *J Therm Anal Calorim*. 2016;126(2):421–33.
46. Otero M, Sánchez ME, Gómez X. Co-firing of coal and manure biomass: a TG–MS approach. *Bioresource Technol*. 2011;102(17):8304–9.
47. Yılmaz MS, Kalpaklı Y, Pişkin S. Thermal behavior and dehydroxylation kinetics of naturally occurring sepiolite and bentonite. *J Therm Anal Calorim*. 2013;114(3):1191–9.
48. Wang Q, Wang HG, Sun BZ, Bai JR, Guan XH. Interactions between oil shale and its semi-coke during Co-combustion. *Fuel*. 2009;88(8):1520–9.
49. Otero M, Calvo LF, Gil MV, Garcia AI, Moran A. Co-combustion of different sewage sludge and coal: a non-isothermal thermogravimetric kinetic analysis. *Bioresour Technol*. 2008;99(14):6311–9.